

Evolution of the jet opening angle distribution in holographic plasma

Krishna Rajagopal, Andrey V. Sadofyev and Wilke van der Schee¹

¹*Center for Theoretical Physics, MIT, Cambridge, MA 02139, USA*

We use holography to analyze the evolution of an ensemble of jets, with an initial probability distribution for their energy and opening angle as in proton-proton (pp) collisions, as they propagate through an expanding cooling droplet of strongly coupled plasma as in heavy ion collisions. We identify two competing effects: (i) each individual jet widens as it propagates; (ii) the opening angle distribution for jets emerging from the plasma within any specified range of energies has been pushed toward smaller angles, comparing to pp jets with the same energies. The second effect arises because small-angle jets suffer less energy loss and because jets with a higher initial energy are less probable in the ensemble. We illustrate both effects in a simple two-parameter model, and find that their consequence in sum is that the opening angle distribution for jets in any range of energies contains fewer narrow and wide jets. Either effect can dominate in the mean opening angle, for not unreasonable values of the parameters. So, the mean opening angle for jets with a given energy can easily shift toward smaller angles, as experimental data may indicate, even while every jet in the ensemble broadens.

I. INTRODUCTION

The discovery that the plasma that filled the microseconds-old universe and that is recreated in nucleus-nucleus collisions at RHIC and the LHC is a strongly coupled liquid poses many outstanding challenges, including understanding how it emerges from an asymptotically free gauge theory that is weakly coupled at short distances. This longer term goal requires understanding how probes of the plasma produced in hard processes in the same collision interact with the plasma, so that measurements of such probes can be used to discern the structure of the plasma as a function of resolution scale. Energetic jets are particularly interesting probes because their formation and subsequent evolution within the plasma involve physics at many length scales.

Although a holographic plasma is strongly coupled at all length scales rather than being asymptotically free, because calculations done via their dual gravitational description can be used to gain reliable understanding of highly dynamical processes at strong coupling these theories have been used to provide benchmarks for various aspects of the dynamics of hard probes propagating through strongly coupled plasma [1–20]. We shall focus on the proxies for light quark jets analyzed in Refs. [9, 17, 19, 21], introducing them into hydrodynamic droplets of plasma whose expansion and cooling resembles that in heavy ion collisions with zero impact parameter, rather than static (slabs of) plasma with a constant temperature. For the first time, we shall analyze an ensemble of such jets with a distribution of jet energies and jet opening angles taken from a perturbative QCD description of jet production in pp collisions. We analyze how this perturbative QCD distribution is modified via tracking how an ensemble of jets in a holographic theory ($\mathcal{N} = 4$ supersymmetric Yang-Mills theory) evolves as the jets propagate through an expanding and cooling droplet of strongly coupled plasma in that

theory, in so doing gaining qualitative insights into how this distribution may be modified in heavy ion collisions, where jets propagate through quark-gluon plasma. (See Refs. [22, 23] for a quite different way to combine weakly coupled calculations of jet production and fragmentation with a holographic, strongly coupled, calculation of parton energy loss into a hybrid model for jet quenching.)

We know from Ref. [19] how the energy and opening angle of an individual jet evolves as it propagates in the strongly coupled $\mathcal{N} = 4$ SYM plasma, at constant temperature. A striking result from this calculation is that all jets with the same initial opening angle (i.e. which would have had the same opening angle if they had been produced in vacuum instead of in plasma) that follow the same trajectory through the plasma suffer the same fractional energy loss, regardless of their initial energy. This highlights the role that the opening angle of a jet plays in controlling its energy loss, a qualitative feature also seen very recently in a weakly coupled analysis of jet quenching in QCD [24], where it can be understood by noting that jets with a larger initial opening angle are jets that have fragmented into more partons, and in particular into more resolved subjet structures, each of which loses energy as it passes through the plasma [25]. The strong dependence of jet energy loss on jet opening angle seen in these analyses shows that the modification of the jet energy distribution due to propagation through the plasma cannot be analyzed in isolation: we must analyze an ensemble of jets with a distribution of both energy and opening angle.

We discern two competing effects. First, as shown for constant-temperature plasma in Refs. [17, 19], the opening angle of every individual jet in the ensemble widens as it propagates through the plasma. The second effect arises because the initial distribution of energies is a rapidly falling function of energy. This means that after the jets have propagated through the plasma, it is more likely that jets with a given final energy are those

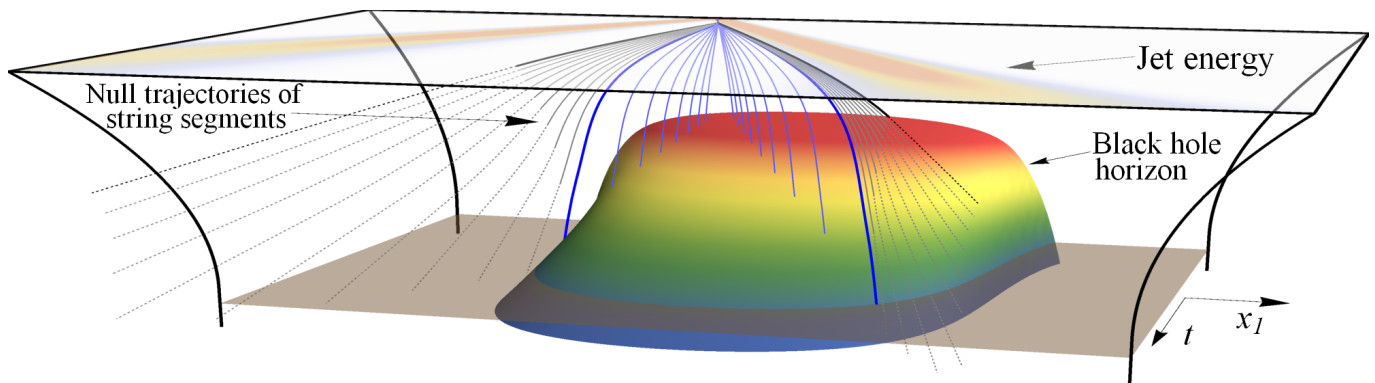


Figure 1. An event where two jets are produced at $x_1 = -3.0$ fm, moving in the $\pm x_1$ directions, with the same initial energy $E_{\text{jet}}^{\text{init}} = 100$ GeV and with the string endpoints (heavier grey curves) moving downward into the AdS bulk with initial angles $\sigma_0 = 0.025$ (0.01) for the left (right) moving jet. The colored profile is the black hole horizon in the AdS bulk, whereby both the height of the surface and its color indicate the temperature as the droplet of plasma expands and cools over time. The droplet is circularly symmetric in the (x_1, x_2) plane; x_2 is not shown. Bits of string follow the grey and blue null trajectories. The lower plane corresponds to the freeze-out temperature; after the temperature drops below this value, we propagate the jet in vacuum and show the constant- σ null rays as dashed. The blue null rays are those that fall into the horizon before freeze-out; the energy propagating along these trajectories is lost from the jet. The heavier blue curve shows the last packet of energy to fall into the horizon, at freeze-out. The opening angle of the jets increase as they traverse the plasma (e.g. for the right-moving jet $\sigma_* = 0.044$, almost 5 times wider than its initial angle) as can be seen from the energy density depicted at the boundary.

that started with only a little more energy and lost little energy rather than being those which started with a much higher energy and lost a lot. Since the narrowest jets lose the least energy [19], propagation through the plasma should push the opening angle distribution of jets with a given energy toward smaller angles. Jets that start out with larger opening angles get kicked down in energy, and become numerically insignificant in the ensemble.

II. THE MODEL

The study of jets in a holographic plasma amounts to the evolution of strings in an anti-de-Sitter (AdS) black hole spacetime with one extra dimension. A pair of light quarks is represented holographically by an open fundamental string in AdS [26] that is governed by the Nambu-Goto action $S = -T_0 \int d\tau d\sigma \sqrt{-h}$, with $T_0 = \sqrt{\lambda}/2\pi$ the string tension, with λ the 't Hooft coupling, τ, σ the string worldsheet coordinates and $h_{ab} = g_{\mu\nu} \partial_a X^\mu \partial_b X^\nu$ the string worldsheet metric, which depends on the metric of the bulk AdS, $g_{\mu\nu}$.

We shall follow Refs. [17, 19] and choose strings that originate at a point at the boundary of AdS, initially propagate as if they were in vacuum [21], and have sufficient energy that they can propagate through the plasma over a distance $\gg 1/T$. As discussed in Ref. [19], after a time $\mathcal{O}(1/T)$ initial transient effects have fallen away. (Literally, in the gravitational description: they fall into the horizon. In the gauge theory, gluon fields around the jet creation event are excited and we need to wait for the jet to separate from gluon fields that are not part of the jet.) After this time, the string has reached a steady-

state regime in which its worldsheet is approximately null and its configuration is specified by two parameters, corresponding in the boundary theory to the initial energy and opening angle of the jet. The endpoint of the string follows a trajectory that initially angles down into the gravitational bulk with an angle σ_0 , see Fig. 1. The initial opening angle of the jet in the boundary gauge theory is (up to few percent corrections) proportional to σ_0 [19]. Once the string is in the steady-state regime, the energy density along the bit of the string with initial downward angle into the bulk σ is given by [17, 19]

$$e(\sigma) = \frac{A}{\sigma^2 \sqrt{\sigma - \sigma_0}}, \quad (1)$$

where the constant A specifies the initial energy of the jet when it enters the steady-state regime, with $E_{\text{jet}}^{\text{init}} \propto A \sigma_0^{-3/2}$ for $\sigma_0 \ll 1$. (A is related to the E_0 of Ref. [19] by $E_0 = 32 \pi^{11/2} A / \Gamma(\frac{1}{4})^6$.) Ideally, we should initialize our strings at a point at the boundary of AdS at $t = 0$ and the initial phase of the calculation should encompass a collision, hydrodynamization of the bulk matter produced therein and, simultaneously, the initial transient dynamics of the string. Details of these early dynamics are not relevant to the qualitative points we wish to make. For simplicity, we shall initialize our strings at a point at the boundary of AdS at $t = 1$ fm/c (when the bulk matter has hydrodynamized), use the steady-state configuration (1) to model the energy density on the string at $t = 1$ fm/c for all σ from σ_0 to $\pi/2$, and take $E_{\text{jet}}^{\text{init}} \equiv \int_{\sigma_0}^{\pi/2} d\sigma e$ as our simplified definition. To specify an ensemble of jets with some distribution of initial energies and opening angles, we must specify an ensemble of strings with the appropriate distribution of A and σ_0 .

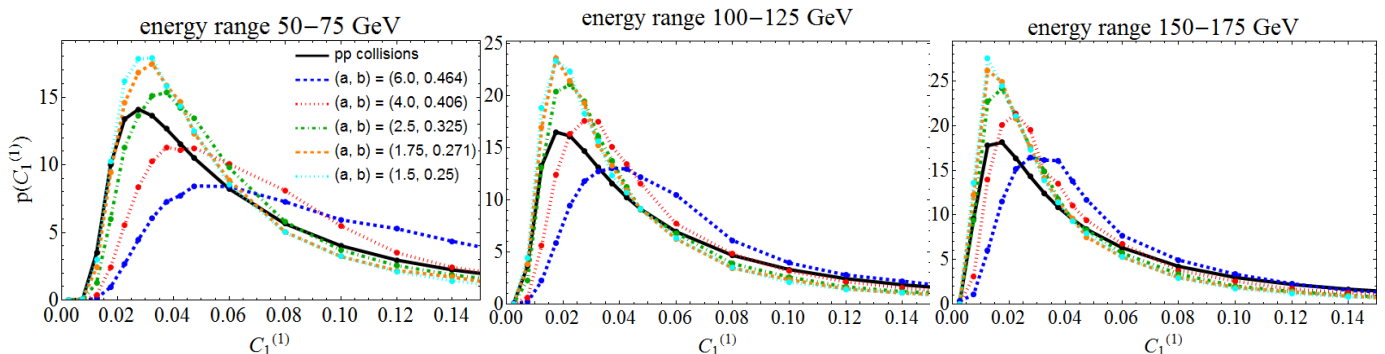


Figure 2. Distribution of the jet opening angle $C_1^{(1)}$ for jets with energies in three bins in pp collisions (black curves) [27]; colored curves show these distributions after an ensemble of jets has propagated through the droplet of plasma, for different choices of model parameters a and b . At small angles, each colored curve has been pushed to the right, to larger angles. At large enough angles, each colored curve has been pushed down, which is equivalent to being pushed to the left. (For the blue curve this happens at larger angles than we have plotted.)

In order to have a distribution that mimics that jets in pp collisions, we choose our distribution of $E_{\text{jet}}^{\text{init}}$ and σ_0 such that the distribution of jet energies is proportional to $(E_{\text{jet}}^{\text{init}})^{-6}$. For our distribution of jet opening angles for jets with a given $E_{\text{jet}}^{\text{init}}$, we use the perturbative QCD calculations of variables denoted $C_1^{(\alpha)}$ that characterize the angular shape of vacuum jets, defined via [27, 28] (see also Refs. [29, 30])

$$C_1^{(\alpha)} \equiv \sum_{i,j} z_i z_j \left(\frac{|\theta_{ij}|}{R} \right)^\alpha, \quad (2)$$

where z_i is the fraction of the jet energy carried by hadron i , θ_{ij} is the angular separation between hadrons i and j , and R is the radius parameter in the anti- k_T reconstruction algorithm [31] used to find and hence define the jets. Setting $\alpha = 1$, the variable $C_1^{(1)}$ is a measure of the opening angle of a jet. We have no analogue of R in our calculation, since we have two known jets per “event”, and hence no analogue of jet finding or jet reconstruction. Somewhat arbitrarily, we shall use $R = 0.3$ in the definition of $C_1^{(1)}$, since the jets in LHC heavy ion collisions whose angular shapes were measured in Ref. [32] were reconstructed with $R = 0.3$. The probability distribution for $C_1^{(1)}$ of quark and gluon jets with a given energy $E_{\text{jet}}^{\text{init}}$ is given by equation (A.8) in Ref. [27], where it has been shown that these distributions compare well with results from PYTHIA, and hence with the distributions for jets produced in pp collisions. We shall use the distributions for quark jets with $R = 0.3$ in pp collisions with $\sqrt{s} = 2.76$ TeV; some sample curves can be seen as the solid curves in Fig. 2.

There is no rigorous connection between σ_0 and $C_1^{(1)}$: our jets are not made of particles, so we have no fragmentation function and no z_i ’s as in the definition (2). However, $C_1^{(1)}$ is a measure of the opening angle of a jet in QCD and from Ref. [19] we know that up to few percent corrections σ_0 is proportional to the opening angle of

the jet, defined there as the half-width at half maximum of the energy flux as a function of angle. Even without the further challenge of connecting to $C_1^{(1)}$, the authors of Ref. [19] advocate that the proportionality constant in this relation should be seen as a free parameter, reflecting differences between jets in a confining theory like QCD and $\mathcal{N} = 4$ SYM. We take

$$C_1^{(1)} = a \sigma_0, \quad (3)$$

with a the first of two free parameters in the specification of our model. (A crude calculation, turning the angular distribution of the energy flux in $\mathcal{N} = 4$ SYM jets [17, 19, 33] into a fictional smooth distribution of many particles all carrying the same small fraction of the jet energy, ignoring the caveats just stated, and applying the definition (2) gives $a \sim 1.7$.)

Finally, we describe the bulk AdS geometry, wherein the string will propagate. We take a metric of the form

$$ds^2 = 2 dt dr + r^2 [-f(r, x_\mu) dt + d\vec{x}_\perp^2 + dz^2], \quad (4)$$

with r the AdS coordinate, and (t, \vec{x}_\perp, z) the field theory coordinates, with z the beam direction. We take $f(r, x_\mu) = 1 - (\pi T(x_\mu) r)^{-4}$, with $T(x_\mu)$ the temperature. This model neglects viscosity and transverse flow. For the temperature profile $T(x_\mu)$, we assume boost invariant longitudinal expansion (a simplification that makes the whole calculation boost invariant, meaning that we need only analyze jets with zero rapidity) and use a simplified blast-wave expression for the transverse expansion [16]

$$T(\tau, \vec{x}_\perp) = b \left[\frac{dN_{\text{ch}}}{dy} \frac{1}{N_{\text{part}}} \frac{\rho_{\text{part}}(\vec{x}_\perp / r_{\text{bl}}(\tau))}{\tau r_{\text{bl}}(\tau)^2} \right]^{1/3}, \quad (5)$$

where $\tau \equiv \sqrt{t^2 - z^2}$ is the proper time, $\rho_{\text{part}}(\vec{x}_\perp)$ is the participant density as given by an optical Glauber model, $N_{\text{part}} \simeq 383$ and $dN_{\text{ch}}/dy \simeq 1870$ [34] are the number of participants and the particle multiplicity at mid-rapidity in 2.76 ATeV 0-5% centrality PbPb collisions at the LHC and $r_{\text{bl}}(\tau) \equiv \sqrt{1 + (v_T \tau / R)^2}$, with

$v_T = 0.6$ and $R = 6.7$ fm. We initialize our calculation at $\tau = 1$ fm/ c , neglecting the initial dynamics via which the hydrodynamic fluid formed and hydrodynamized. The constant b is a measure of the multiplicity per entropy S and, for $S/N_{\text{ch}} \simeq 7.25$ [35, 36] and $S/(T^3V) \simeq 15$ [37, 38] as in QCD at $T \simeq 300$ MeV, is given by $b \simeq 0.78$. (Note that $b = 0.659$ in Ref. [16].) We shall treat b as the second free parameter in our model because the number of degrees of freedom is greater in $\mathcal{N} = 4$ SYM theory than in QCD and the couplings in the theories differ too. We are propagating $\mathcal{N} = 4$ SYM jets through an $\mathcal{N} = 4$ SYM plasma with temperature T meaning that we must use a b that is smaller than the QCD value.

As already noted, for simplicity we initialize our jets at $\tau = 1$ fm/ c , when we initialize the plasma. We choose the initial position in the transverse plane of our jets according to a binary scaling distribution, proportional to $\rho_{\text{part}}(\vec{x}_\perp)^2$, and choose their transverse direction of propagation randomly. For a given choice of our two model parameters a and b , we generate an ensemble of jets with their initial position and direction distributed as just described and their initial energy and opening angle (σ_0 in the dual gravitational description) distributed as described above.

We then allow each string in the ensemble to propagate in AdS, as we have illustrated for a sample dijet in Fig. 1. We compute the energy loss by integrating the string energy that falls into the black hole (along the blue curves in Fig. 1) before its temperature has fallen to a freeze-out temperature that we set to 175 MeV (defined with $b = 0.78$ so that our freeze-out time is reasonable). We assume that once the temperature has dropped below freeze-out, the string that remains propagates in vacuum (along the dashed grey curves in Fig. 1) meaning that the angle at which the string endpoint travels downward into the AdS bulk no longer changes. This final angle, which we denote σ_* , describes the opening angle of the jet that emerges from the droplet of plasma, $C_1^{(1)} = a\sigma_*$. In this way, we extract the energy and opening angle of each of the jets from among the initial ensemble that emerge from the droplet of plasma. We can then obtain the modified probability distribution of jet energies and opening angles in the final-state ensemble. (We did the calculation by first evolving many tens of thousands of jets with varying values of their initial energy, opening angle, transverse position and direction and constructing an interpolating function giving the final energy and final opening angle as a function of these four input variables. We repeated this for each chosen value of b . For each value of a , we then reweighted these interpolating functions according to the desired probability distribution for the four input variables, and sampled from the reweighted final-state distributions in order to obtain the results that we shall present below.)

Recapitulating, we have a two parameter model that describes how the distribution of jet energies and open-

ing angles changes due to the propagation of the jets through an expanding, cooling droplet of strongly coupled plasma relative to what that distribution would be in a pp collision. The model parameter a sets the relationship between the downward angle followed by the string endpoint trajectory in the gravitational description (initially, σ_0 ; after propagation through the plasma, σ_*) and the jet opening angle $C_1^{(1)}$ — whose initial distribution we have taken from perturbative QCD and whose final distribution we have computed. The model parameter b controls the relationship between the temperature of the $\mathcal{N} = 4$ SYM plasma in our model and that of the QCD plasma we are modeling. Larger b results in a stronger gravitational pull on the string, meaning greater energy loss and a greater increase in the opening angle of every jet in the ensemble.

III. RESULTS AND DISCUSSION

We illustrate our results in Figs. 2 and 3 for five combinations of the model parameters a and b . In Fig. 2, we show how the probability distribution for the jet opening angle $C_1^{(1)}$ is modified via propagation through the plasma. In Fig. 3, we show that our combinations of a and b each yield the same suppression in the number of jets with a given energy in the final ensemble relative to that in the initial ensemble, R_{AA}^{jet} . The effect on R_{AA}^{jet} of increasing a can be compensated by increasing b : increasing a means reducing the σ_0 of the strings corresponding to jets with a given $C_1^{(1)}$; this reduces their energy loss, which is compensated by increasing b . It is striking is how differently the $C_1^{(1)}$ distributions in Fig. 2 and the $\langle C_1^{(1)} \rangle$ in Fig. 3 are modified with the different combinations of a and b .

There are two effects affecting the probability distribution for the jet opening angle. First, as in Fig. 1, each null geodesic curves down, so all jets become wider [17, 19]. And, the larger b is, meaning the larger the $\mathcal{N} = 4$ SYM temperature T in the calculation, the stronger the gravitational force in AdS, the more the geodesics curve down, and the more the jet opening angle distribution shifts to larger angle. We see exactly this effect in Fig. 2, at all but large values of the opening angle $C_1^{(1)}$. Second, jets with a smaller σ_0 and hence a smaller initial opening angle lose fractionally less energy [19]. This means that jets that initially had larger values of the opening angle $C_1^{(1)}$ lost more energy and got kicked out of the energy bin corresponding to their panel in Fig. 2, depleting this large-angle region of the distribution. This region of the distribution can get repopulated with jets that started out with substantially higher energy, but because the initial energy distribution goes like $(E_{\text{jet}}^{\text{init}})^{-6}$ there are not enough of these jets to combat the depletion. This depletion effect becomes more significant the larger the value

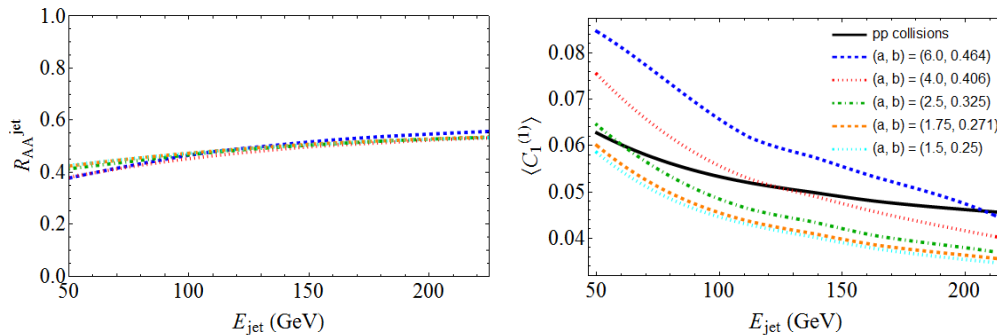


Figure 3. Colored curves show R_{AA}^{jet} (left) and the ensemble average of the jet opening angle, $\langle C_1^{(1)} \rangle$, (right) for the final ensemble of jets after propagation through the droplet of plasma, for the same combinations of a and b as in Fig. 2. Here, R_{AA}^{jet} is the ratio of the number of jets with a given energy after propagation through the plasma to that in the initial ensemble. This quantity from our model should not be compared quantitatively to experimental measurements of R_{AA} for either hadrons or jets as we have no hadrons, no background, no multi-jet events, and no jet finding or reconstruction. However, we have chosen combinations of a and b such that R_{AA}^{jet} is similar in all cases, and is similar to R_{AA} for jets in LHC heavy ion collisions [39–41]. Even though R_{AA}^{jet} is so similar for all the colored curves, the opening angle distributions (Fig. 2) and their mean $\langle C_1^{(1)} \rangle$ (right) vary significantly. We have also plotted $\langle C_1^{(1)} \rangle$ for the unperturbed ensemble, as in pp collisions (black curve).

of σ_0 , meaning that as the model parameter a is reduced the $C_1^{(1)}$ above which the depletion is significant comes down, as seen in Fig. 2. In Fig. 3 (right) we show the ensemble average of the jet opening angle $C_1^{(1)}$. We see that the combinations of a and b that we have chosen that all yield comparable R_{AA}^{jet} can result in either one or the other of the two salient effects illustrated in Fig. 2 being dominant, meaning that propagation through the plasma can result in $\langle C_1^{(1)} \rangle$ increasing or decreasing.

There are of course many ways in which one could improve our model. Collisions with nonzero impact parameter and nontrivial longitudinal dynamics could be included, as could viscous hydrodynamics, realistic transverse and longitudinal flow, and jets with nonzero rapidity. One could attempt to model effects on the jet of physics during the first fm/ c of the collision and after freezeout, both of which we have neglected, or to consider an ensemble of quark jets and gluon jets. And, one can imagine choosing probability distributions for other observables (dijet asymmetries; $C_1^{(\alpha)}$ for $\alpha \neq 1$) from data on pp collisions or perturbative QCD calculations and studying how these distributions are modified in an ensemble of jets that has propagated through the droplet of plasma produced in a heavy ion collision.

Our hope is that, even given its simplifications, our work can address qualitative aspects of jet shape modifications, as for instance seen by CMS [32, 42]. There, it is noticed that jets in heavy ion collisions are somewhat narrower than jets with the same energy in pp collisions, if one focuses on particles within the jets that are either close to the jet axis or have $p_T > 4$ GeV. Reconstructing jets incorporates soft particles at large angles originating from the wake of moving plasma trailing behind the jet rather than from the jet itself; focusing on jet modifications at smaller angles or higher p_T therefore makes sense. It is tempting to conclude that the reduction in

$\langle C_1^{(1)} \rangle$ due to the greater energy loss suffered by jets with a larger initial opening angle may be the dominant effect seen in these data. This would point toward values of a and b in the lower half of the range that we have explored, where the depletion at large angles dominates and the mean opening angle of jets with a given energy decreases even while every jet in the ensemble broadens.

Remarkably, almost independent of the values of our model parameters our model provides a clear qualitative prediction. When comparing the angular distributions of pp collisions with AA collisions, as done in Fig. 2, we see that the distribution almost always has fewer jets with the smallest and the largest opening angles, with the depletion at small angles due to the broadening of the jets in the ensemble and the depletion at large angles originating as described above. Whether the mean opening angle goes up or down depends on which effect dominates but, regardless, we expect the distribution of the opening angles of jets in AA collisions to be narrower than in pp collisions. The striking qualitative features of the results we have already obtained from our admittedly simplified model provide strong motivation for analyzing the distribution of jet opening angles, as well as its mean, in other models for jet quenching, in Monte Carlo calculations of jet quenching at weak coupling, and in analyses of data.

Acknowledgments: We thank Jorge Casalderrey-Solana, Paul Chesler, Andrej Ficnar, Doga Gulhan, Simone Marzani, Guilherme Milhano, Daniel Pablos and Jesse Thaler for useful discussions. We are especially grateful to Simone Marzani for providing formulae from Ref. [27]. Research supported by the U.S. Department of Energy under grant Contract Number DE-SC0011090.

-
- [1] C. Herzog, A. Karch, P. Kovtun, C. Kozcaz, and L. Yaffe, *JHEP* **0607**, 013 (2006), hep-th/0605158.
- [2] H. Liu, K. Rajagopal, and U. A. Wiedemann, *Phys. Rev. Lett.* **97**, 182301 (2006), hep-ph/0605178.
- [3] J. Casalderrey-Solana and D. Teaney, *Phys. Rev.* **D74**, 085012 (2006), hep-ph/0605199.
- [4] S. S. Gubser, *Phys.Rev.* **D74**, 126005 (2006), hep-th/0605182.
- [5] H. Liu, K. Rajagopal, and U. A. Wiedemann, *Phys. Rev. Lett.* **98**, 182301 (2007), hep-ph/0607062.
- [6] M. Chernicoff, J. A. Garcia, and A. Guijosa, *JHEP* **09**, 068 (2006), hep-th/0607089.
- [7] S. S. Gubser, *Nucl.Phys.* **B790**, 175 (2008), hep-th/0612143.
- [8] J. Casalderrey-Solana and D. Teaney, *JHEP* **04**, 039 (2007), hep-th/0701123.
- [9] P. M. Chesler, K. Jensen, A. Karch, and L. G. Yaffe, *Phys.Rev.* **D79**, 125015 (2009), 0810.1985.
- [10] S. S. Gubser, D. R. Gulotta, S. S. Pufu, and F. D. Rocha, *JHEP* **0810**, 052 (2008), 0803.1470.
- [11] P. Arnold and D. Vaman, *JHEP* **10**, 099 (2010), 1008.4023.
- [12] P. Arnold and D. Vaman, *JHEP* **04**, 027 (2011), 1101.2689.
- [13] P. M. Chesler, Y.-Y. Ho, and K. Rajagopal, *Phys. Rev.* **D85**, 126006 (2012), 1111.1691.
- [14] A. Ficnar and S. S. Gubser, *Phys.Rev.* **D89**, 026002 (2014), 1306.6648.
- [15] P. M. Chesler, M. Lekaveckas, and K. Rajagopal, *JHEP* **1310**, 013 (2013), 1306.0564.
- [16] A. Ficnar, S. S. Gubser, and M. Gyulassy, *Phys. Lett.* **B738**, 464 (2014), 1311.6160.
- [17] P. M. Chesler and K. Rajagopal (2014), 1402.6756.
- [18] R. Morad and W. A. Horowitz, *JHEP* **11**, 017 (2014), 1409.7545.
- [19] P. M. Chesler and K. Rajagopal (2015), 1511.07567.
- [20] J. Casalderrey-Solana and A. Ficnar (2015), 1512.00371.
- [21] P. M. Chesler, K. Jensen, and A. Karch, *Phys.Rev.* **D79**, 025021 (2009), 0804.3110.
- [22] J. Casalderrey-Solana, D. C. Gulhan, J. G. Milhano, D. Pablos, and K. Rajagopal, *JHEP* **1410**, 19 (2014), 1405.3864.
- [23] J. Casalderrey-Solana, D. C. Gulhan, J. G. Milhano, D. Pablos, and K. Rajagopal (2015), 1508.00815.
- [24] J. G. Milhano and K. C. Zapp (2015), 1512.08107.
- [25] J. Casalderrey-Solana, Y. Mehtar-Tani, C. A. Salgado, and K. Tywoniuk, *Phys. Lett.* **B725**, 357 (2013), 1210.7765.
- [26] A. Karch and E. Katz, *JHEP* **0206**, 043 (2002), hep-th/0205236.
- [27] A. J. Larkoski, S. Marzani, G. Soyez, and J. Thaler, *JHEP* **05**, 146 (2014), 1402.2657.
- [28] A. J. Larkoski, G. P. Salam, and J. Thaler, *JHEP* **06**, 108 (2013), 1305.0007.
- [29] A. Banfi, G. P. Salam, and G. Zanderighi, *JHEP* **03**, 073 (2005), hep-ph/0407286.
- [30] M. Jankowiak and A. J. Larkoski, *JHEP* **06**, 057 (2011), 1104.1646.
- [31] M. Cacciari, G. P. Salam, and G. Soyez, *JHEP* **04**, 063 (2008), 0802.1189.
- [32] S. Chatrchyan et al. (CMS Collaboration), *Phys. Lett.* **B730**, 243 (2014), 1310.0878.
- [33] Y. Hatta, E. Iancu, A. H. Mueller, and D. N. Triantafyllopoulos, *JHEP* **02**, 065 (2011), 1011.3763.
- [34] E. Abbas et al. (ALICE Collaboration), *Phys. Lett.* **B726**, 610 (2013), 1304.0347.
- [35] B. Muller and K. Rajagopal, *Eur.Phys.J.* **C43**, 15 (2005), hep-ph/0502174.
- [36] S. S. Gubser, S. S. Pufu, and A. Yarom, *Phys.Rev.* **D78**, 066014 (2008), 0805.1551.
- [37] S. Borsanyi, Z. Fodor, C. Hoelbling, S. D. Katz, S. Krieg, and K. K. Szabo, *Phys. Lett.* **B730**, 99 (2014), 1309.5258.
- [38] A. Bazavov et al. (HotQCD), *Phys. Rev.* **D90**, 094503 (2014), 1407.6387.
- [39] S. Chatrchyan et al. (CMS Collaboration) (2012), CMS PAS HIN-12-004.
- [40] G. Aad et al. (ATLAS Collaboration), *Phys. Rev. Lett.* **114**, 072302 (2015), 1411.2357.
- [41] J. Adam et al. (ALICE Collaboration), *Phys. Lett.* **B746**, 1 (2015), 1502.01689.
- [42] S. Chatrchyan et al. (CMS) (2015), CMS-PAS-HIN-15-011.